Frontiers in Heat and Mass Transfer

Tech Science Press

https://doi.org/10.32604/fhmt.2026.079339

ARTICLE

Underground Thermal Energy Storage of Corn Stover Combustion Heat for Grain Drying and Home Heating

Berry Lamy*, Romaine Byfield and Yiding Cao

Department of Mechanical and Materials Engineering, Florida International University, Miami, FL, USA

*Corresponding Author: Berry Lamy. Email: blamy002@fiu.edu

Received: 20 January 2026; Accepted: 15 April 2026; Published: 29 June 2026

ABSTRACT: Climate change and the ongoing dependence on fossil fuels present major challenges for global agriculture, with fossil fuel use in the agrifood sector accounting for a substantial and growing share of greenhouse gas (GHG) emissions. Agrifood systems currently contribute approximately one-third of total anthropogenic GHG emissions. Integrating renewable energy solutions for heating and power can help offset a significant fraction of these emissions. In this study, an analytical heat transfer and thermodynamic model is developed to evaluate the performance, energy balance, and thermal losses of the proposed system under realistic operating conditions. The model enables quantitative assessment of heat storage efficiency and long-term thermal retention. Using a representative 800 ha Iowa corn farm as a case study, the analysis shows that combustion of sustainably harvested corn stover (30% removal rate) can provide approximately 9.60 TJ of useful seasonal heat with a plausible range of 6.2 to 18.5 TJ depending on yield, moisture content, and conversion parameters. Thermal analysis of an underground hot water storage for agricultural applications shows that over a storage period of 200 days, the temperature reduction of the stored hot water can be less than 10%. Since the analytical model conservatively neglects container liner and concrete resistances, the actual thermal retention in an engineered system would likely be equal to or better than this estimate. This level of performance is sufficient to meet the seasonal grain-drying and building heating demands on a large Iowa corn farm in a year.

KEYWORDS: Thermal energy storage (TES); underground thermal energy storage (UTES); biomass combustion; corn stover; Iowa

1 Introduction

The State of Iowa, at the heart of the United States (U.S.) corn belt, may hold the solution to alleviate the agriculture industry's dependence on fossil fuels and offset carbon emissions. Each year, Iowa's vast corn (*Zea mays*) harvest generates large amounts of agricultural corn stover residues (husks, cobs, etc.) that are traditionally left on the fields to decompose, a practice which helps to replenish the soil with essential nutrients such as Nitrogen (N) and to prevent soil erosion. Graham et al. [1] have found that up to 30% of the corn stover can be collected annually for less than $30 per dry ton with little to no negative impact on soil health or erosion rates [1,2]. In many years, the volume of these agricultural byproducts matches or even surpasses the weight of the harvested corn grain itself, resulting in surplus residues for which farmers often have no direct use [3].

Agriculture is an energy-intensive industry, and Iowa's farmers rely heavily on fossil fuels such as propane and diesel to power essential seasonal operations. Of particular concern are the energy demand for grain drying following the fall harvest and greenhouse heating during Iowa's cold winter, both of which are

not only critical to farm productivity but are also subject to volatile fuel prices and supply shortages. In recent years, farmers have increasingly faced exposure to energy market volatility: demand in harvest season for propane can strain distribution systems and sharply raise fuel costs, which in turn jeopardize time-sensitive post-harvest drying or storage operations. While the degree of exposure varies by region and farming system (e.g., those with better logistics or access to renewables are less vulnerable), reliance on fossil fuels remains a structural economic risk for many agricultural operations. Moreover, the CO_2 emissions from fossil fuel combustion in agriculture (direct on-farm energy use) cannot be ignored, though in many agroecosystems the largest emission sources remain non-CO_2 (e.g., methane, nitrous oxide).

Using heat generated by the controlled combustion of corn stover in a biomass furnace, farms may be able to turn what was traditionally considered agricultural waste into a lucrative, sustainable energy resource [4]. This biomass combustion process can be used with the Utility-Scale Underground Hot-Water Storage (USUHWS), an underground thermal energy storage (UTES) technology by Cao [5], to provide thermal energy storage for year-round use. Thermal energy generated by biomass burning can be efficiently stored underground during the harvest season, when crop leftovers are at their peak. During winter, stored heat is available for use during the winter months, when energy demand for grain drying and greenhouse heating is highest. In addition, the stored heat can be used to heat the home. Leveraging Iowa's surplus corn residues for renewable energy, along with subsurface thermal energy storage, is a novel approach to increasing energy independence, lowering greenhouse gas emissions, and fostering economic resilience in rural areas.

Globally, agrifood systems contribute to about 30% (around 16.5 billion t of CO_2 in 2023) of anthropogenic greenhouse gas (GHG) emissions [6]. The agricultural sector is both highly vulnerable to climate change and a major contributor to it. Together, agriculture, forestry, and land use account for roughly 25% of global GHG emissions, as shown in Table 1 [7]. Although the efficiency of agricultural production has greatly improved since the 1970s, absolute emissions have continued to rise with growing demand, and there are signs energy efficiency gains at the farm level may be stagnating [8–10]. This trend suggests that the increasing energy demand of agriculture cannot be met by technological advancements in machinery and management alone.

Table 1: Global emissions by each economic sector [7].

Emission Sources	Percentage
Agricultural, forestry, and other land uses	25%
Buildings	6%
Electricity and heat	25%
Industries including chemical, metallurgical, and mineral extraction	21%
Transportation	14%
Other energy	9%

Continued reliance on fossil fuels in agriculture has dire consequences. Rising fuel costs increase production expenses, which ultimately raises food prices for consumers. Supply disruptions, whether from geopolitical instability, climate-related disasters, or infrastructure failures, can further destabilize food systems. In the long term, this unsustainable reliance on fossil fuels threatens both food security and rural economic vitality [11]. To address this challenge, the agricultural sector must adopt renewable energy sources, efficient machinery, and improved management practices to significantly reduce the energy use from fossil

fuels [12–14]. The key technologies involved in renewable energy transition include sources such as solar, wind, hydro, and bioenergy, as well as advanced energy storage technologies [15].

1.1 Biomass Combustion

When biomass, like corn stover, is burned, its chemical energy is released and converted into usable thermal energy. Based on the latent heat of vaporization (2.44 GJ per tonne of water removed at 25°C) as the sole component of the total heat of desorption, the energy required to dry 500 t of corn grain from 25% to 15% wet basis is estimated to be approximately 122 GJ [16,17].

The emission factors are 0.15833 tCO_2e/GJ for electricity, 0.07254 tCO_2e/GJ for diesel, 0.06124 tCO_2e/GJ for propane, and 0.05069 tCO_2e/GJ for natural gas (CNG) [17].

The process involves several processes, each with its own efficiency factor, which determines how much of the original energy is ultimately available for useful work.

$$\dot{Q}_{fuel}\,(\mathrm{t}) = \frac{\mathrm{dQ_{fuel}}}{dt} = -\frac{dm_{bs}}{dt} \times (1 - X_m) \times HHV \tag{1}$$

where $\dot{Q}_{fuel}$ is the instantaneous heat release rate of corn stover biomass (dry basis) in W, m_{bs} is the mass of the biomass (wet basis) in kg, X_m is the moisture fraction of the biomass, and HHV is the higher heating value of dry biomass in MJ/kg_{dry}.

If we assume that combustion is complete, Eq. (1) can be written as Eq. (2) below in terms of total fuel energy:

$$Q_{fuel} = m_{bs} \times (1 - X_m) \times HHV \tag{2}$$

However, if the combustion is not complete, a combustion efficiency should be included in the calculation of combustion heat:

$$Q_{comb} = Q_{fuel} \times \eta_{comb} \tag{3}$$

Q_{comb} is the energy released by combustion and η_{comb} is the combustion efficiency. In general, the combustion efficiency is rather high, close to 100%.

In this kind of combustor, a boiler is not needed because the purpose of the combustor is to produce hot water for storage using the released combustion heat. However, not all the combustion heat can be used to produce hot water for storage, and the heat exchanger efficiency is thus considered. Thus, the total thermal energy that is delivered to the storage can be calculated by the following relation:

$$Q_{in} = Q_{comb} \times \varepsilon_{hx} \tag{4}$$

In the above equation, ε_{hx} is the heat exchanger effectiveness, which is used to produce hot water. The final relation for the total thermal energy acquired by the hot water may be calculated by the following relation:

$$Q_{in} = m_{bs} \times (1 - X_m) \times HHV \times \eta_{comb} \times \varepsilon_{hx} \tag{5}$$

Shah et al. (2011) found that for uncovered stover stored outside for short durations, the moisture fraction, X_m, is about 18% (18 wt%). Table 2, from Cantrell et al. [18], summarizes HHV for different corn stover fractions on a dry basis. The whole stover HHV is 17.26 MJ/kg_{dry} which is the value consistently

throughout this study. Using a base-case combustion efficiency of η_{comb} = 0.88 and a heat-exchanger effectiveness of ε_{hx} = 0.80 (sensitivity ranges of 0.85–0.95 and 0.75–0.90, respectively, are discussed later), the useful heat delivered per kilogram of harvested wet biomass is:

$$\frac{Q_{in}}{m_{bs}} = (1 - 0.18)\left(17.26\frac{\text{MJ}}{\text{kg}}\right)(0.82)\,(0.70) \approx 8.12\,\text{MJ/kg}_{\text{wet}} \tag{6}$$

Table 2: Higher heating value (HHV) of corn stover at 0% moisture [18].

Part	Mean Higher Heating Value (HHV) (MJ/kg_{dry})	Standard Deviation (STD)
Below, below ear	17.93	0.37
Bottom, leaves	17.78	0.34
Bottom, stalk	17.55	0.40
Cob	18.25	0.28
Top, above ear	18.06	0.24
Top, leaves	17.63	0.14
Top, stalk	17.79	0.30
Whole stover plant	17.26	0.43

Research by Wojcieszak et al. [19] confirms corn stover faction heating values fall in the range of 17.7 to 18.2 MJ/kg, consistent with Cantrell et al. [18] values used in this study. For every megawatt-hour of energy produced from biomass, energy-related emissions are reduced by nearly 0.5 t of CO_2 equivalent relative to propane. Biomass combustion technologies, such as direct combustion, gasification, and combined heat and power (CHP) systems, have become increasingly efficient, enabling agricultural byproducts to be converted into usable electricity and heat for farming operations or nearby industries [12].

1.2 Underground Thermal Energy Storage: Background and Context

Underground Thermal Energy Storage (UTES) systems have been widely recognized as efficient and cost-effective solutions for storing thermal energy, particularly in building and geothermal applications. Recent studies have provided comprehensive analyses of system configurations, including linear, spiral, and slinky heat exchanger designs, along with detailed evaluations of thermodynamic performance under varying geometric, material, and climatic conditions [20].

Wei et al. [21] conducted a comprehensive knowledge-graph analysis of 7705 UTES publications spanning 1990–2024 and identified rising interest in high-temperature storage systems and multi-energy complementarity. Zhang et al. [22] reviewed the development status of UTES, noting critical challenges such as injection blockage, wellbore scaling, and seepage heat transfer that must be addressed for large-scale deployment. However, existing research largely overlooks the integration of biomass-based energy sources and application-specific deployment in agricultural systems. There is limited work coupling agricultural residues, such as corn stover, with underground thermal storage, and few studies develop analytical heat transfer and thermodynamic models that capture the full energy pathway from generation to storage and end-use. Additionally, seasonal agricultural energy demands, and associated carbon reduction potential remain insufficiently addressed.

To bridge these gaps, this study develops an analytical heat transfer and thermodynamic framework for a biomass-integrated Utility-Scale Underground Hot-Water Storage (USUHWS) system, with a focus on farm-scale, seasonal energy storage and sustainable agricultural applications.

1.3 Biomass Energy Production Coupled with USUHWS

Biomass combustion of corn stover offers significant potential for supplying useful energy to the agricultural sector. However, realizing this potential requires an effective seasonal storage mechanism, because the residue supply and combustion opportunity are concentrated in the post-harvest autumn window, while the dominant thermal demands (grain drying continuation, building heating) extend through winter. Without such storage, the full benefits of biomass energy cannot be captured.

The USUHWS [5] provides a sealed, pressurized underground hot-water storage vessel that is well-suited to store heat for extended periods with moderate thermal losses. By integrating USUHWS with a biomass combustion system, agricultural operations can benefit from a reliable, scalable, and seasonally matched energy storage pathway. Fig. 1 depicts the overall system schematic.

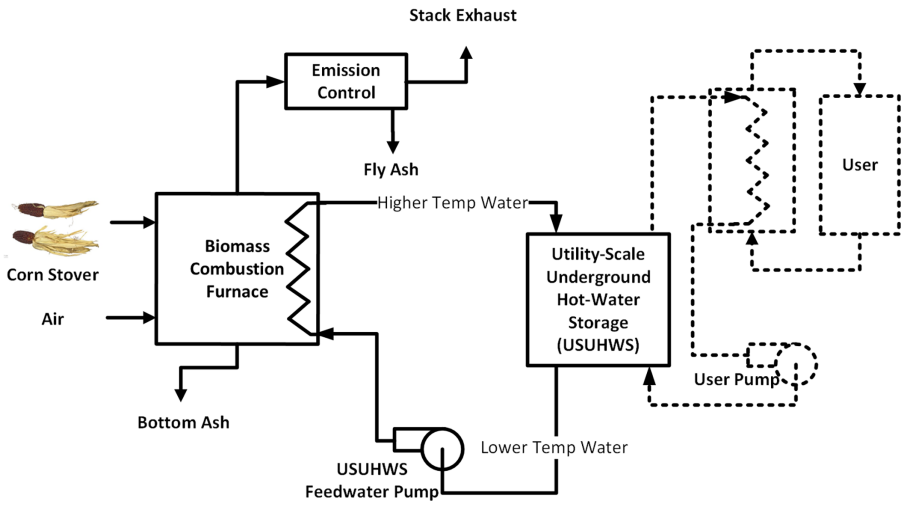

Figure 1: Schematic of biomass combustion charged USUHWS.

2 Case Study

To demonstrate heat storage potential at a practical maximum capacity, this study uses a farm surface area of 8 km^2 (800 ha or 1977 acres), representing the upper end of large commercial corn farms in Iowa. This scale is consistent with Iowa State University findings that large commercial farms averaged 1930 acres (781 ha) in 2021 [23]. In addition, the 2022 USDA Census of Agriculture indicates that Iowa had 6449 farms between 500–1999 acres (202 to 809 ha) and 446 farms with 2000 acres (809 ha) or more that harvested corn for grain, confirming that operations in this size range represent a significant segment of Iowa's large-scale agricultural sector [24].

The analysis is intentionally framed as a feasibility study and therefore uses a single transparent base-case parameter set together with low-high sensitivity bounds. Table 3 consolidates the principal geometric, biomass, thermal, and operating assumptions used in this study.

Table 3: Consolidated base-case assumptions and sensitivity ranges.

Parameter	Base Value	Range/Source Basis	Role in Analysis
Farm area	800 ha	Case-study assumption from large Iowa farm scale	Biomass supply basis
Dry stover yield	4.0 t/ha	3.5–4.5 t/ha from literature [25]	Available residue
Stover removal fraction	0.30	0.25–0.40 sensitivity band [1,26]	Sustainably removable feedstock
Moisture fraction, X_m	0.18	Shah et al. [27]; short duration outside storage	Wet-basis correction
HHV (dry basis)	17.26 MJ/kg	Whole-stover value from Table 2 [18]	Fuel energy content
η_{comb} (combustion eff.)	0.88	0.85–0.95 sensitivity band	Fuel energy to combustion heat
ε_{hx} (HX effectiveness)	0.80	0.75–0.90 sensitivity band	Combustion heat to storage water
Storage temperature, T_0	150°C	Meets all farm thermal loads (Table 4)	Charging target
Far-field soil temperature, T_∞	12°C	Annual mean for central Iowa	Heat-sink temperature
Soil thermal conductivity, k_s	0.75 W/(m·K)	0.5, 0.75, 1.0 W/(m·K) cases [28]	External loss parameter
Burial depth to cylinder center, d	10 m (base)	6–20 m sensitivity cases	External resistance/ground pressure
Tank geometry	Cylinder, L = 100 m	Radius from required volume	Storage configuration

The typical dry corn stover production in this region is about 3.5 to 4.5 t/ha (317,514.75 to 408,233.25 kg/km^2) [25]. While no-till harvesting technique and corn-corn rotation allow for a greater amount of harvestable stover (nearly 50%), a sustainable removal rate of 30% is selected to maintain soil health and prevent erosion [26]. Using the base-case useful heat value of approximately 9.98 MJ/kg$_{wet}$ and a representative dry stover yield of 4.0 t/ha with a moisture content of 18%, the farm-scale useful thermal energy available for storage is approximately 9.51 TJ. A broader plausible range is summarized in Table 5.

The maximum available wet stover mass for biomass combustion, m_{bs}, using 4.0 t/ha dry yield and 18% moisture content:

$$m_{bs} = \frac{(800\,\text{ha})\left(4.0\frac{\text{tons}}{\text{ha}}\right)(0.3)}{(1-0.18)} = 1,170,732\ \text{kg(wet)} \tag{7}$$

Using Eq. (5) with the base-case parameters from Table 3, the total useful seasonal thermal energy available from the case-study farm is:

$$Q_{in} = (1,170,732\,\text{kg})(1-0.18)\left(17.26\frac{\text{MJ}}{\text{kg}}\right)(0.82)(0.70) \approx 9.51\,\text{TJ} \tag{8}$$

This value should be interpreted as a first-order seasonal heat budget rather than a guaranteed annual delivery. Actual recoverable energy will depend on weather, stover collection efficiency, storage losses during biomass handling, and combustor operating conditions. The uncertainty band is addressed in Table 5.

Following combustion of corn stover for heat generation, the residual ash may be returned to the field as a soil amendment. Research has demonstrated that biomass ash contains significant concentrations of plant-available nutrients, particularly potassium and phosphorus, which can substitute for a portion of synthetic fertilizer applications. The ash also exhibits liming properties due to its alkaline nature, effectively neutralizing soil acidity and improving the availability of nutrients such as nitrogen and phosphorus [29,30]. Additional benefits include the supply of secondary nutrients (Ca, Mg, S) and micronutrients (Fe, Mn, Zn, Cu, B, Mo) that support optimal crop growth and yield [31].

Table 4: Typical temperature requirements for common heat applications on a farm.

Application	Typical Max Temperature (°C)	Source
Home space heating (radiators, hydronic)	60–80	[32]
Domestic hot water	50–70	[33]
Corn drying	80–110	[34]
Greenhouse heating	40–60	[32,35]

Table 5: Uncertainty band for useful thermal energy and required storage.

Case	Yield (t/ha dry)	Removal Fraction	Moisture X_m	$\eta_{comb}/\varepsilon_{hx}$	Useful Heat (TJ)	Equiv. Volume (m^3)
Low	3.5	0.25	0.20	0.85/0.75	~6.2	~11,600
Base	4.0	0.30	0.18	0.88/0.80	~9.6	~18,000
High	4.5	0.40	0.15	0.92/0.88	~18.5	~34,800

2.1 Storage Volume

Table 4 shows typical temperature requirements for common heating applications on a farm. Based on this table, a maximum storage temperature of 150°C is used in this study, which is sufficient for home heating, domestic hot water through heat exchange, greenhouse heating, and indirect hot-air grain drying. Operating at this temperature also keeps the system within the range of pressurized liquid-water storage commonly considered for high-temperature hot-water systems. Table 6 shows water Temperatures and corresponding saturation pressures. As can be seen at a storage temperature of about 150°C, the hot water could accomplish required heating applications while requiring moderate pressure loading for storage containers.

Table 6: Water temperatures and corresponding saturation pressures [36].

Temperature (°C)	Saturation Pressure (bar)
100	1.01
120	1.99
150	4.76
180	10.02
200	15.54
250	39.75

To calculate the required storage-water volume, the total useful energy from biomass combustion is equated to the sensible thermal energy stored in pressurized liquid water. The base case therefore uses the useful thermal energy value after both combustion and heat-exchange losses have been applied once, consistent with Eq. (5).

To calculate the required volume of water, V_{HW}, for underground energy storage, the total energy available from the combustion of corn stover is equated to the thermal energy that can be stored in the water (shown in Eqs. (9) and (10)). The density of hot water is ρ_{HW}, and the specific heat capacity of hot water is $c_{p,HW}$. The ambient temperature is T_∞, corresponding to the temperature of the water entering the combustor, by assuming that the initial water temperature in the storage chamber is close to the ambient temperature. $T_{\max}$ is the hot-water temperature exiting the combustor and entering the storage chamber.

At a storage temperature of 150°C, the water density and specific heat are approximately ρ_{HW} = 917 kg/m^3 and $c_{p,HW}$ = 4200 J/(kg·K), respectively. For an ambient temperature of 12°C, a useful thermal inventory of $Q_{in} \approx 9.51$ TJ, and an initial-to-reference temperature difference of (150 − 12) = 138°C, the required storage volume is approximately 1.8×10^4 m^3, as shown below:

$$Q_{in} = (\rho_{HW} * V_{HW}) * c_{p,HW} * (T_{\max} - T_\infty) \tag{9}$$

$$V_{HW} = \frac{Q_{in}}{\rho_{HW} * c_{p,HW} * (T_{\max} - T_\infty)} \tag{10}$$

$$V_{HW} = \frac{9.51\,\text{TJ}}{\left(917\frac{\text{kg}}{\text{m}^3}\right) * \left(4200\frac{\text{J}}{\text{kgK}}\right) * (423.15\,\text{K} - 285.15\,\text{K})} = 17{,}893.0\,\text{m}^3 \tag{11}$$

2.2 Storage System Geometry

For underground hot water storage, the cylindrical shape is chosen as the best configuration because of a number of important benefits. First, this geometry enables the storage of a greater volume of water per unit footprint compared to other shapes, which maximizes the efficiency of land use and storage capacity. The reduced surface area for a given volume translates to less soil that must be removed during installation, resulting in lower labor and machinery expenses. Another important benefit of the cylindrical design is the even distribution of pressure along the container walls. This uniformity allows for the use of thinner walls, which in turn means less construction material is required without compromising structural integrity. Furthermore, because a cylinder has a lower surface area relative to its volume, it experiences reduced heat loss. This characteristic significantly improves energy retention within the storage system, enhancing overall performance.

Using a cylindrical structure, V_{HW} can be rewritten in terms of internal radius r and length L:

$$\pi r^2 L = V_{HW} \tag{12}$$

$$r = \sqrt{\frac{V_{HW}}{\pi * L}} \tag{13}$$

For a length, L = 100 m. The minimum diameter, r is given below:

$$r = \sqrt{\frac{18,000\ \mathrm{m}^3}{\pi * 100\ \mathrm{m}}} = 7.57\ \mathrm{m} \tag{14}$$

2.3 Thermal Analysis of the Storage System

Eq. (15) shows an energy balance of the storage system: The rate of change of thermal energy stored within the storage system $\dot{E}_{st}$ the rate of thermal energy entering the storage $\dot{E}_{in}$ the rate of the energy leaving the storage system $\dot{E}_{out}$. The rate of change of thermal energy stored within the storage system can be estimated by Eq. (16), assuming the temperature in the storage is uniform. To assess the capacity of the storage system to maintain the energy content of stored energy over a sufficiently long time, $\dot{E}_{in}$ is assumed to be zero (Eq. (17)) and the energy leaving the storage is only due to the energy loss to the surrounding soil (Eq. (18)), where U is the overall heat transfer coefficient between the stored hot water and the surrounding soil, and A is the associated heat transfer area.

$$\dot{E}_{st} = \dot{E}_{in} - \dot{E}_{out} \tag{15}$$

To assess thermal retention during the storage phase (no charging), $\dot{E}_{in} = 0$, and:

$$\dot{E}_{st} = mc_{p,HW}\frac{dT(t)}{dt} = (\rho_{HW} * V_{HW} * c_{p,HW})\frac{dT(t)}{dt} = -\dot{E}_{out} = -UA(T(t) - T_\infty) \tag{16}$$

$$\dot{E}_{out} = \dot{Q}_{loss} = UA(T(t) - T_\infty) \tag{17}$$

where U is the overall heat transfer coefficient, A is the associated heat transfer area, and $T(t)$ is the bulk water temperature at time t.

The thermal resistance network between the stored hot water and the far-field soil includes: (1) internal water-side convection, (2) calcium-silicate liner conduction, (3) concrete wall conduction, and (4) soil conduction to the far-field. The present analytical model retains only the dominant soil resistance in order to focus the analysis on the key external loss term and to produce a conservative (lower-bound) estimate of thermal retention. An order-of-magnitude justification follows.

For the base-case geometry ($r \approx 7.6$ m, L = 100 m, k_s = 0.75 W/(m·K), burial depth d = 10 m), the external soil resistance computed from Eq. (23) is approximately $R_{soil} \approx 2 \times 10^{-3}$ K/W. By comparison, a 50 mm calcium-silicate liner ($k \approx 0.06$ W/(m·K)) contributes approximately $R_{liner} \approx 1.7 \times 10^{-4}$ K/W; a structural concrete wall ($k \approx 1.5$ W/(m·K), 200 mm thick) contributes approximately $R_{concrete} \approx 10^{-5}$ to 10^{-4} K/W; and an internal water-side convection coefficient above about 500 W/(m^2·K) gives $R_{conv} \approx 4 \times 10^{-6}$ K/W. Thus, soil resistance dominates by roughly an order of magnitude over the next largest resistance (the liner). Neglecting the non-soil resistances is therefore a conservative simplification, because including them would predict lower total heat losses.

Fig. 2 shows schematically the buried cylindrical storage system, where k_s is the effective soil thermal conductivity, L is the cylinder length, and T_∞ is the far-field soil temperature. The governing buried-cylinder heat-loss relation assumes predominantly radial, quasi-steady conduction into a semi-infinite surrounding

soil domain with an approximately constant far-field temperature. These assumptions are appropriate for a first-order feasibility estimate, but they omit seasonal soil-temperature drift and local moisture-dependent changes in soil conductivity.

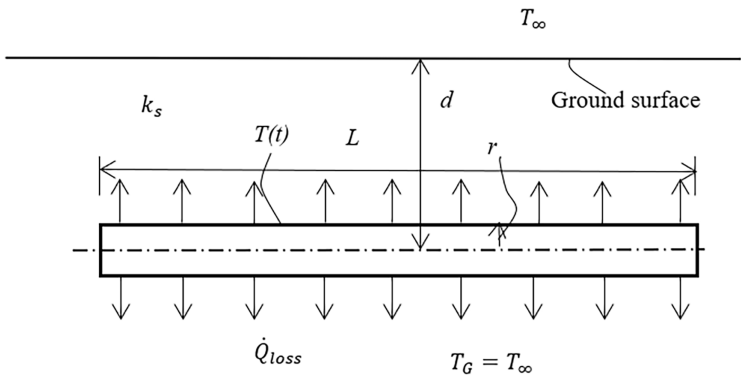

Figure 2: Schematics of an underground cylindrical storage system of the present design.

Fig. 2 shows schematically an underground cylindrical storage system of the present design, where k_s is the effective soil thermal conductivity, L is the length of storage cylinder, T is the average temperature of the hot water, which is also the outer surface temperature of the container after the thermal resistances from the hot water to the container are neglected, T_G is the undisturbed surrounding earth temperature that can take the ambient air temperature for simple calculation [28], d is the distance from the ground surface to the centerline of the storage cylinder, and r is the radius of the storage cylinder.

The governing buried-cylinder heat-loss relation assumes predominantly radial, quasi-steady conduction into a semi-infinite surrounding soil domain with an approximately constant far-field temperature [31]. According to Kusuda [28] and Cao [37], the heat loss from the storage cylinder can be calculated by the following equation:

$$\dot{Q}_{loss} = \frac{2\pi k_s L(T - T_\infty)}{\ln\left(\frac{d}{r} + \sqrt{\left(\frac{d}{r}\right)^2 - 1}\right)} \tag{18}$$

where k_s is the effective soil thermal conductivity, L is the cylinder length, T is the bulk hot-water temperature, T_∞ is the undisturbed far-field soil temperature (approximated as the annual mean air temperature), d is the depth from the ground surface to the cylinder center, and r is the cylinder radius [31]. These assumptions are appropriate for a first-order feasibility estimate but omit seasonal soil-temperature drift and local moisture-dependent changes in soil thermal conductivity; these effects would be quantified in a detailed site-specific design.

The above equation (Eq. (18)) can be rewritten as:

$$\dot{Q}_{loss} = \frac{2\pi k_s L(T - T_\infty)}{\ln\left(\frac{d}{r} + \sqrt{\left(\frac{d}{r}\right)^2 - 1}\right)} = \frac{(T - T_\infty)}{\ln\left(\frac{d}{r} + \sqrt{\left(\frac{d}{r}\right)^2 - 1}\right) \Big/ (2\pi k_s L)} = \frac{(T - T_\infty)}{R_{tot}} \tag{19}$$

$$R_{tot} = \ln\left(\frac{d}{r} + \sqrt{\left(\frac{d}{r}\right)^2 - 1}\right) \Big/ (2\pi k_s L) \tag{20}$$

According to the definition of UA,

$$UA = \frac{1}{R_{tot}} = \frac{(2\pi k_s L)}{\ln\left(\frac{d}{r} + \sqrt{\left(\frac{d}{r}\right)^2 - 1}\right)} \tag{21}$$

Substituting Eq. (21) into Eq. (16) and letting:

$$C = -\frac{(2\pi k_s L)}{\ln\left(\frac{d}{r} + \sqrt{\left(\frac{d}{r}\right)^2 - 1}\right)} \times \frac{1}{\rho_{HW} * V_{HW} * c_{p,HW}} \tag{22}$$

Eq. (16) can be written as:

$$\frac{dT(t)}{dt} = \frac{d[T(t) - T_\infty]}{dt} = \mathrm{C} \times (\mathrm{T}(t) - T_\infty) \tag{23}$$

Let

$$y = T(t) - T_\infty \tag{24}$$

A differential equation in terms of y can be written as:

$$\frac{dy}{dt} = \mathrm{C} \times y \tag{25}$$

Separating the variables of y and t and integrating the equation between $t = 0$ and $t = t$, we have

$$\int_{y(0)}^{y(t)} \frac{dy}{y} = \int_0^t C dt \tag{26}$$

$$\ln\left(\frac{y(t)}{y(0)}\right) = C \times t \tag{27}$$

Take antilog:

$$\frac{y(t)}{y(0)} = e^{Ct} \tag{28}$$

or

$$y(t) = y(0) \times e^{Ct} \tag{29}$$

Substituting back the definition of y, we have:

$$T(t) - T_\infty = (T(0) - T_\infty) \times e^{Ct} \tag{30}$$

where $T(0)$ is the initial bulk storage temperature at $t = 0$ and $C = -UA/(\rho_{HW} \times V_{HW} \times c_{p,HW})$. This lumped-capacitance model assumes that the water body behaves as a thermally mixed (uniform temperature) mass. For a large tank, some thermal stratification is expected in practice. Stratified operation would generally reduce effective losses from the hottest region and improve the deliverable outlet temperature

during discharge. Accordingly, the present formulation should be interpreted as a conservative mixed-tank approximation rather than a validated transient CFD description. Stratified-tank modeling is recommended for future design stages.

In Eq. (30), $T(0)$ is the initial hot water or the storage temperature at $t = 0$, and $T(t)$ is the storage temperature after a storage time period of t.

The variation of storage temperature is governed primarily by soil thermal conductivity and burial depth because these parameters control the dominant external resistance. In this study, the influence of k_s and d are examined parametrically, while r, L, and $T(0)$ are held at base-case values. Table 7 lists all storage container parameters used.

Table 7: Storage container parameters (base case).

Symbol	Value	Units	Description
ρ_{HW}	917	kg/m^3	Density of water inside the storage tank at 150°C
$c_{p,HW}$	4200	J/(kg·K)	Specific heat capacity of hot water at 150°C
r	7.58	m	Radius of the storage tank
L	100	m	Length of the storage tank
d	10–20	m	Soil depth from the ground surface
k_s	0.5 to 1.0	W/(m·K)	Thermal conductivity of soil [28]
T_∞	≈12	°C	Temperature of the environmental air
$T(0)$	150	°C	Initial hot water temperature

2.4 Temperature Decay in the Storage System

Based on Eq. (30) and the parameters in Table 7, Fig. 3 shows the bulk storage temperature over 200 days under three different soil thermal conductivities (0.5, 0.75, and 1.0 W/(m·K)) with burial depth held constant at d = 10 m. Fig. 4 shows the temperature evolution for three burial depths (10, 15, and 20 m) with k_s = 0.75 W/(m·K). A 200-day storage duration is considered sufficient to span the nominal period between post-harvest charging and the end of winter heating demand for Iowa agricultural operations. The conservative analytical model (neglecting liner, concrete, and insulation resistances) predicts that over 200 storage days the bulk water temperature decline remains below approximately 10% of the initial 150°C storage temperature for burial depths of 10 m and deeper. Because the model neglects the additional resistances that would be present in an engineered system, this result should be interpreted as a lower-bound estimate of thermal retention; a detailed engineered system incorporating intentional insulation, a stratified operating mode, and optimized liner design would likely perform at least as well and potentially better.

The demand side can be roughly estimated for comparison. Grain drying of approximately 1000 t of corn with a 5 percentage-point moisture reduction requires on the order of 3–5 TJ [34], while a farmhouse or small greenhouse heating load over a heating season would be on the order of tens to hundreds of GJ, well within the base-case storage inventory of 9.51 TJ. This order-of-magnitude comparison confirms that the calculated storage capacity is large enough to justify further design study, although exact supply-demand matching will depend on specific crop throughput, dryer type, greenhouse area, and heat delivery system design.

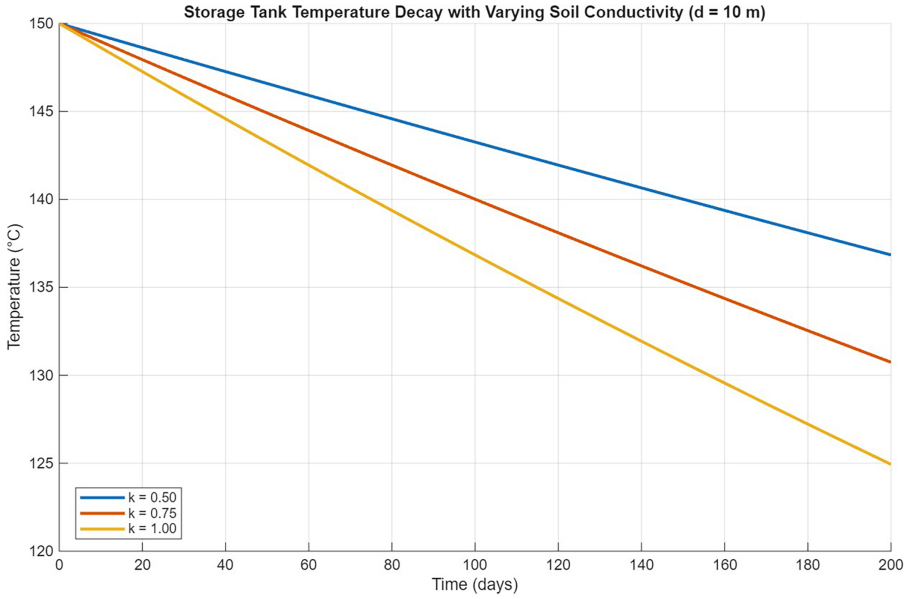

Figure 3: Storage tank temperature change over 200 storage days at three different soil thermal conductivities while soil depth d is held at 10 m.

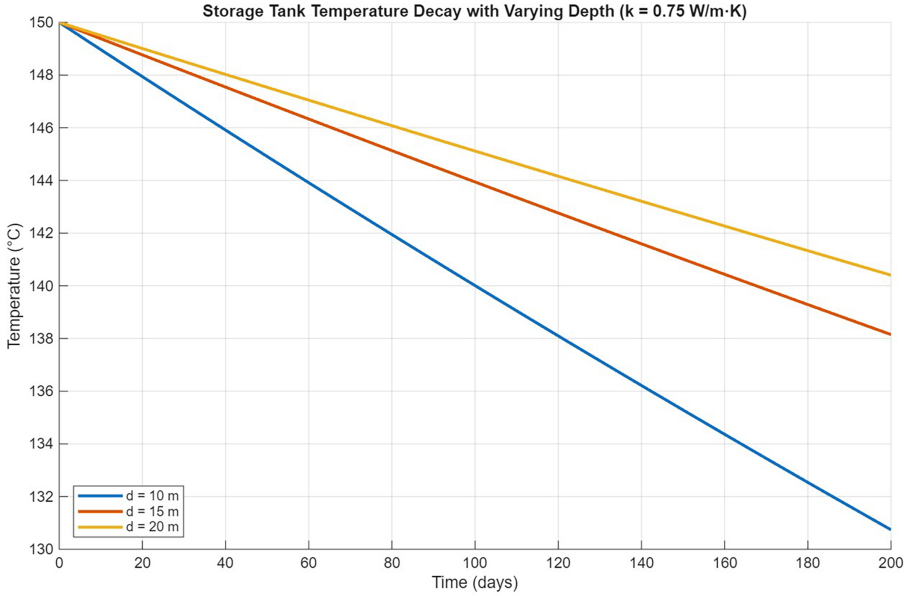

Figure 4: Storage tank temperature change over 200 storage days with varying soil depths while the soil thermal conductivity is held at 0.75 W/m·K.

2.5 Pumping and Stress

The proposed system requires continuous water circulation between the biomass combustion unit, the Utility-Scale Underground Hot-Water Storage (USUHWS), and the end-use load, resulting in pumping energy penalties that must be considered in overall system efficiency. These penalties arise primarily from overcoming frictional losses in piping, minor losses due to fittings, and any elevation head differences.

Given the large storage volume and expected high flow rates required for heat exchange, pumping power can be estimated from:

$$P_{pump} = \frac{\rho g Q H}{\eta} \tag{31}$$

where Q is volumetric flow rate, H is total dynamic head, and η is pump efficiency.

The structural design of the USUHWS must account for both hydrostatic pressure and thermal-induced stresses associated with storing water at elevated temperatures. This internal pressure generates hoop (circumferential) stress in the concrete wall, which can be approximated by:

$$\sigma_{hoop} = \frac{Pr}{t} \tag{32}$$

where P is internal pressure and t is wall thickness.

In addition to internal pressure, the structure must withstand external soil burden and thermal expansion effects. However, since this study is focused on evaluating the feasibility of the USUHWS concept for the proposed application, detailed analysis of pumping energy requirements, structural reinforcement, and pressure containment will be addressed in future work.

2.6 Operating Mode and Pressure Management

The intended operating mode is a sealed, pressurized hot-water storage vessel charged and discharged in a single-phase liquid regime, not a deliberately vented boiling tank. During charging, dissolved and entrained air would be removed using conventional high-point vents and a controlled deaeration procedure so that oxygen inventory is minimized while the vessel remains liquid-filled. The internal pressure is then governed by a combination of the saturation pressure corresponding to the hot-water temperature, the static liquid head, and the pressure-control strategy of the charging loop. Maintaining single-phase liquid water avoids flashing, unstable two-phase flow, and degraded pump performance at the delivery side.

Because the base-case storage temperature is 150°C, the system would require a pressure-management strategy such as a pressurizer, expansion volume, relief devices, and appropriate code-compliant containment. Pumping power is not included in the present thermal budget, but it would be a secondary parasitic load associated with long piping runs, charging duration, and flow-rate selection and should be quantified in later design stages.

As shown in Table 6, the saturation pressure at 150°C is approximately 4.76 bar. The absolute pressure at depth h below the water surface within the storage container is:

$$p_{abs}(h) = p_{sat}(T_{\max}) + \rho g h \tag{33}$$

$$p_{gauge}(h) = p_{abs}(h) - p_{atm} \tag{34}$$

Fig. 5 illustrates the internal pressure distribution with depth. This pressure profile represents only part of the structural loading on the storage vessel. The final structural design must account for hydrostatic pressure, thermal stress, external soil and groundwater loads, restraint effects, code-based safety factors for pressurized water service, and potential fatigue from repeated charge–discharge cycles. These requirements reinforce that the present work should be treated as an initial screening study, not a final design.

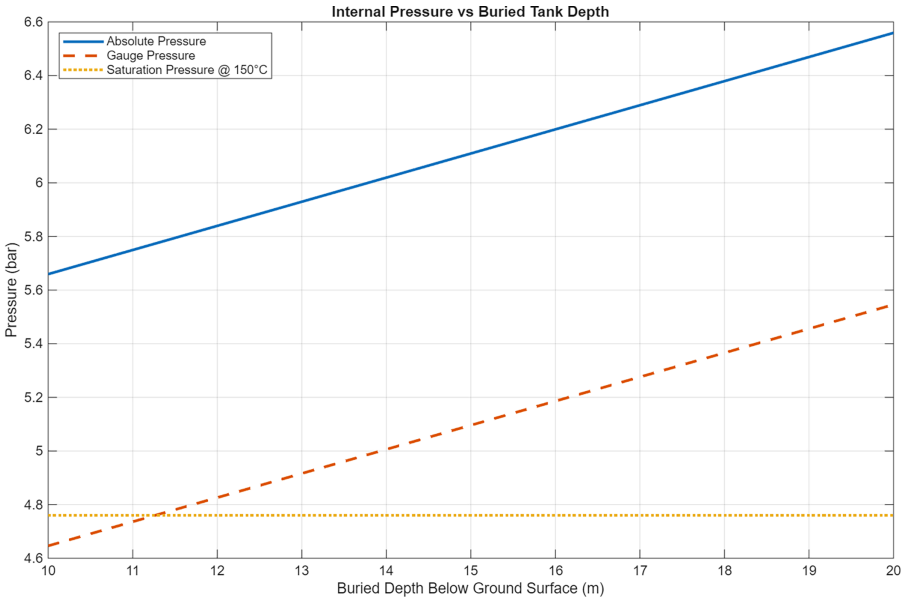

Figure 5: Internal pressure at varying depth.

2.7 Uncertainty Band: Thermal Energy and Storage Volume

The results reported above are base-case point estimates. Because the principal input parameters stover yield, removal fraction, moisture content, combustion efficiency, and heat-exchanger effectiveness are all subject to natural variability, Table 5 provides a simple low-base-high sensitivity band.

3 Discussion and Conclusions

This paper is positioned as a feasibility study rather than a validated final design. Practical implementation would require a combustion system large enough to charge roughly 9.6 TJ over the available post-harvest window, which implies careful selection of furnace scale, heat-exchanger surface area, ash handling, particulate and emissions control, and stover collection and moisture-management logistics. Future work should couple the present analytical framework to detailed charging schedules, pumping-power estimates, CFD or stratified-tank analysis, structural design of the pressurized vessel, finite-element heat-transfer modeling, and experimental validation.

1. Biomass combustion, when integrated with the USUHWS system, presents a practical option for displacing fossil fuels in Iowa agricultural operations. The concept is particularly attractive where crop residue is already available on site and where seasonal heating loads, grain drying and building heating are otherwise served by propane or diesel.
2. For a representative 800 ha Iowa corn farm, the base-case calculation indicates approximately 9.6 TJ of useful seasonal thermal energy from corn stover at a 30% removal rate, with a plausible uncertainty band of approximately 6.2–18.5 TJ (Table 5). This is large enough to cover realistic on-farm grain-drying and heating loads, providing a strong incentive for further design study.
3. The conservative analytical heat-loss model predicts that the bulk water temperature declines by less than 10% of its initial 150°C value over 200 storage days for the burial depths studied. Because the model neglects container liner, concrete, and insulation resistances, this is a conservative lower-bound estimate; actual thermal retention in a properly engineered system would be equal to or better than predicted here. The lumped-capacitance thermal model is a conservative simplification for a tank of this scale.

In practice, thermal stratification would reduce losses from the hottest region and improve deliverable outlet temperature. Stratified-tank or CFD analysis is recommended for future design stages. Practical implementation would require: (a) a combustion system large enough to charge approximately 9.6 TJ over the available post-harvest window (implying careful selection of furnace scale, heat-exchanger surface area, and stover handling logistics); (b) ash handling and particulate/emissions control for biomass combustion; (c) a pressure-management system appropriate for pressurized 150°C hot-water service; and (d) stover collection, densification, and moisture-management logistics.

4. Structural analysis of the storage container is essential. The pressure profile shown in Fig. 5 represents only part of the mechanical loading. The final design must combine hydrostatic pressure, thermal stress, external soil and groundwater loads, code-based safety provisions, and fatigue considerations for high-temperature pressurized water service.
5. This study concentrates on analytical feasibility evaluation. For a comprehensive design, both Finite Element Analysis (FEA) of the structural vessel and experimental validation of the thermal performance are essential next steps. Future work should couple the present analytical framework to detailed charging schedules, pumping-power estimates, stratified-tank analysis, and economic cost modeling.

Acknowledgement: Not applicable.

Funding Statement: The authors received no specific funding.

Author Contributions: The authors confirm contribution to the paper as follows: Conceptualization, Berry Lamy and Yiding Cao; methodology, Berry Lamy; software, Berry Lamy; validation, Berry Lamy, Romaine Byfield and Yiding Cao; formal analysis, Berry Lamy; investigation, Berry Lamy; resources, Berry Lamy; data curation, Berry Lamy; writing and original draft preparation, Berry Lamy; writing, review and editing, Romaine Byfield and Yiding Cao; visualization, Berry Lamy; supervision, Yiding Cao. All authors reviewed and approved the final version of the manuscript.

Availability of Data and Materials: Not applicable.

Ethics Approval: Not applicable.

Conflicts of Interest: The authors declare no conflicts of interest.

Nomenclature

t	Time, s
d	Soil layer depth, m
L	Length of storage cylinder, m
k_s	Soil thermal conductivity
r	Radius of storage cylinder
V_{HW}	Volume of hot water in storage
m_{bs}	Mass of biomass (kg, wet basis)
X_m	Moisture fraction of biomass
HHV	Higher heating value of dry biomass
η_{comb}	Combustion efficiency
ε_{hx}	Heat-exchanger effectiveness
$c_{p,HW}$	Specific heat of water
UA	Tank overall loss coefficient
$T(t)$	Tank bulk temperature
T_∞	Ambient temperature
ρ_{HW}	Density, Water

ρ_s	Density, Soil
m^3	Cubic meter
km^3	Square Kilometer
TJ	Terrajules
UTES	Underground thermal energy storage
USUHWS	Utility-Scale Underground Hot-Water Storage
GHG	Greenhouse Gas
CHP	Combined Heat and Power
N	Nitrogen
CO_2	Carbon dioxide
ha	Hectares
tCO_2e/GJ	Tonnes of CO_2 equivalent per gigajoule

References

1. Graham RL, Nelson R, Sheehan J, Perlack RD, Wright LL. Current and potential U.S. corn stover supplies. Agron J. 2007;99(1):1–11. doi:10.2134/agronj2005.0222.
2. Malone RW, Herbstritt S, Ma L, Richard TL, Cibin R, Gassman PW, et al. Corn stover harvest N and energy budgets in central Iowa. Sci Total Environ. 2019;663:776–92. doi:10.1016/j.scitotenv.2019.01.328.
3. Tyndall JC, Berg EJ, Colletti JP. Corn stover as a biofuel feedstock in Iowa's bio-economy: an Iowa farmer survey. Biomass Bioenergy. 2011;35(4):1485–95. doi:10.1016/j.biombioe.2010.08.049.
4. Soltero V, Chacartegui R, Ortiz C, Lizana J, Quirosa G. Biomass district heating systems based on agriculture residues. Appl Sci. 2018;8(4):476. doi:10.3390/app8040476.
5. Cao Y. An ultimate solution to phasing out fossil fuels—part I: utility-scale underground hot-water storage (USUHWS) for power production and heat supply. Front Heat Mass Transf. 2022;19:1–12. doi:10.5098/hmt.19.1.
6. FAO. Greenhouse gas emissions from agrifood systems. Rome, Italy: Food and Agriculture Organization of the United Nations; 2025. doi:10.4060/cd7300en.
7. Intergovernmental Panel on Climate Change (IPCC). Climate change 2022—mitigation of climate change: working group III contribution to the sixth assessment report of the intergovernmental panel on climate change. Cambridge, UK: Cambridge University Press; 2023. doi:10.1017/9781009157926.
8. Parton WJ, Gutmann MP, Merchant ER, Hartman MD, Adler PR, McNeal FM, et al. Measuring and mitigating agricultural greenhouse gas production in the US Great Plains, 1870–2000. Proc Natl Acad Sci U S A. 2015;112(34):E4681–8. doi:10.1073/pnas.1416499112.
9. Martinho VJPD. Energy consumption across European Union farms: efficiency in terms of farming output and utilized agricultural area. Energy. 2016;103(4):543–56. doi:10.1016/j.energy.2016.03.017.
10. Bennetzen EH, Smith P, Porter JR. Agricultural production and greenhouse gas emissions from world regions—the major trends over 40 years. Glob Environ Change. 2016;37:43–55. doi:10.1016/j.gloenvcha.2015.12.004.
11. Peduzzi P, Harding Rohr Reis R. The end to cheap oil: a threat to food security and an incentive to reduce fossil fuels in agriculture. Environ Dev. 2012;3:157–65. doi:10.1016/j.envdev.2012.05.008.
12. Rahman MM, Mostafiz BS, Paatero JV, Lahdelma R. Extension of energy crops on surplus agricultural lands: a potentially viable option in developing countries while fossil fuel reserves are diminishing. Renew Sustain Energy Rev. 2014;29(2):108–19. doi:10.1016/j.rser.2013.08.092.
13. Paris B, Vandorou F, Balafoutis AT, Vaiopoulos K, Kyriakarakos G, Manolakos D, et al. Energy use in open-field agriculture in the EU: a critical review recommending energy efficiency measures and renewable energy sources adoption. Renew Sustain Energy Rev. 2022;158:112098. doi:10.1016/j.rser.2022.112098.
14. Arévalo P, Ochoa-Correa D, Villa-Ávila E, Espinoza JL, Albornoz E. Decarbonizing insular energy systems: a literature review of practical strategies for replacing fossil fuels with renewable energy sources. Fuels. 2025;6(1):12. doi:10.3390/fuels6010012.
15. Kabeyi MJB, Olanrewaju OA. Sustainable energy transition for renewable and low carbon grid electricity generation and supply. Front Energy Res. 2022;9:743114. doi:10.3389/fenrg.2021.743114.

16. Panigrahi SS, Singh CB, Fielke J. A 3D transient CFD model to predict heat and moisture transfer in on-farm stored grain silo through parallel computing using compiler directives: impact of discretization methods on solution efficacy. Dry Technol. 2023;41(7):1133–47. doi:10.1080/07373937.2022.2121284.
17. Panigrahi SS, Luthra K, Singh CB, Atungulu G, Corscadden K. On-farm grain drying system sustainability: current energy and carbon footprint assessment with potential reform measures. Sustain Energy Technol Assess. 2023;60(1103–11):103430. doi:10.1016/j.seta.2023.103430.
18. Cantrell KB, Novak JM, Frederick JR, Karlen DL, Watts DW. Influence of corn residue harvest management on grain, stover, and energy yields. BioEnergy Res. 2014;7(2):590–7. doi:10.1007/s12155-014-9433-9.
19. Wojcieszak D, Przybył J, Czajkowski Ł, Majka J, Pawłowski A. Effects of harvest maturity on the chemical and energetic properties of corn stover biomass combustion. Materials. 2022;15(8):2831. doi:10.3390/ma15082831.
20. Le Roux D, Noël H, Fuentes A, Colinart T. Review on horizontal underground thermal energy storage (HUTES). J Energy Storage. 2026;147(1):119927. doi:10.1016/j.est.2025.119927.
21. Wei R, Li Y, Liu Y. Progress in underground thermal energy storage: research contents, hotspots, and development trends. Appl Energy. 2025;401(Suppl 1):126725. doi:10.1016/j.apenergy.2025.126725.
22. Zhang YN, Liu YG, Bian K, Zhou GQ, Wang X, Wei MH. Development status and prospect of underground thermal energy storage technology. J Groundw Sci Eng. 2024;12(1):92–108. doi:10.26599/jgse.2024.9280008.
23. Peters D. ISU rural Iowa at a glance [Internet]. 2022 [cited 2026 Apr 2]. Available from: https://smalltowns.soc.iastate.edu/wp-content/uploads/sites/504/2025/04/SOC3104C_2022.pdf.
24. USDA. Census of agriculture. Washington, DC, USA: United States Department of Agriculture; 2024.
25. Gent S, Twedt M, Gerometta C, Almberg E. Introduction to feedstocks. In: Theoretical and applied aspects of biomass torrefaction. Amsterdam, The Netherlands: Elsevier; 2017. p. 17–39. doi:10.1016/b978-0-12-809483-9.00002-6.
26. Battaglia M, Thomason W, Fike JH, Evanylo GK, von Cossel M, Babur E, et al. The broad impacts of corn stover and wheat straw removal for biofuel production on crop productivity, soil health and greenhouse gas emissions: a review. GCB Bioenergy. 2021;13(1):45–57. doi:10.1111/gcbb.12774.
27. Shah A, Darr MJ, Webster K, Hoffman C. Outdoor storage characteristics of single-pass large square corn stover bales in Iowa. Energies. 2011;4(10):1687–95. doi:10.3390/en4101687.
28. Kusuda T. Heat transfer analysis of underground heat and chilled-water distribution systems. Gaithersburg, MD, USA: National Institute of Standards and Technology; 1981. doi:10.6028/NBS.IR.81-2378.
29. Ackerman DJ, Cicek N. Recovering agricultural nutrients (potassium and phosphorus) from biomass ash: a review of literature. Winnipeg, MB, Canada: University of Manitoba; 2017. doi:10.13140/RG.2.2.24745.85605.
30. Bang-Andreasen T, Nielsen JT, Voriskova J, Heise J, Rønn R, Kjøller R, et al. Wood ash induced pH changes strongly affect soil bacterial numbers and community composition. Front Microbiol. 2017;8:1400. doi:10.3389/fmicb.2017.01400.
31. Przygocka-Cyna K, Barłóg P, Spiżewski T, Grzebisz W. Bio-fertilizers based on digestate and biomass ash as an alternative to commercial fertilizers—the case of tomato. Agronomy. 2021;11(9):1716. doi:10.3390/agronomy11091716.
32. Nemali K. Temperature control in greenhouses, 2021 [Internet]. [cited 2026 Apr 2]. Available from: https://www.extension.purdue.edu/extmedia/HO/HO-327-W.pdf.
33. National Academies of Sciences, Engineering, and Medicine. Management of legionella in water systems. Washington, DC, USA: National Academies Press; 2019. doi:10.17226/25474.
34. Maier DE, Bakker-Arkema FW. Grain drying systems. In: Proceedings of the 2002 Facility Design Conference of the Grain Elevator & Processing Society (GEAPS FDC); 2002 Jul 28–31; St. Charles, IL, USA.
35. Coradi PC, Maldaner V, Lutz É, da Silva Daí PV, Teodoro PE. Influences of drying temperature and storage conditions for preserving the quality of maize postharvest on laboratory and field scales. Sci Rep. 2020;10(1):22006. doi:10.1038/s41598-020-78914-x.
36. Incropera. Fundamentals of heat and mass transfer. 5th ed. Hoboken, NJ, USA: John Wiley & Sons, Inc.; 2002.
37. Cao Y. An ultimate solution to phasing out fossil fuels—part II: air-water thermal power plants for utility-scale power production at low temperatures. Front Heat Mass Transf. 2022;19:1–16. doi:10.5098/hmt.19.2.